

Modification of Diamond Conditioner with V-SAM Coatings for Corrosion Prevention During Metal CMP

Byoung-Jun Cho, R. Prasanna Venkatesh, Tae-Young Kwon and Jin-Goo Park*

Department of Bio-nano and Materials Engineering, Hanyang University, Ansan, Korea

*E-mail: jgpark@hanyang.ac.kr

Received: 28 January 2013 / Accepted: 5 March 2013 / Published: 1 April 2013

In the present work, the vapor phase-self assembled monolayers made from two different precursors, 1-dodecanethiol (DT) and perfluorooctyltrichlorosilane (FOTS), were prepared on a nickel surface under optimized conditions [2]. The various properties of the coating surfaces during exposure to an aqueous solution were evaluated and compared with a bare nickel surface through electrochemical analyses such as potentiodynamic polarization and electrochemical impedance spectroscopy (EIS). Potentiodynamic polarization studies revealed that these coatings inhibit both anodic and cathodic reactions as both the E_{corr} and I_{corr} values of the coating surfaces decrease. An electrical equivalent circuit (EEC) model is employed to analyze the impedance data. The protection efficiency of these coatings when exposed to commercial Cu and W slurry were also evaluated. Ni with a V-SAM coating showed good corrosion resistance against Cu slurry. However, these coatings could not provide adequate protection to an underlying Ni layer against exposure to W slurry. Thus, the base Ni layer was replaced with a Ni alloy (palladium-nickel-chrome) and V-SAM coatings were prepared using the same two precursors. These coatings showed high protection efficiency, even against the highly acidic W slurry. In addition, fluorocarbons of various thicknesses deposited on Ni and Ni alloys by a plasma polymerization technique showed higher corrosion resistance to the W slurry. Contact angle measurements were also used to assess the structural integrity of the coatings.

Keywords: CMP, Ni, PNC, V-SAM coatings, Plasma polymerization

1. INTRODUCTION

Metal chemical mechanical polishing (CMP) is one of the key processes used in semiconductor manufacturing industries to planarize metal surfaces such as Cu, W, Ta, and Ru [1,2]. During this process, pressure is applied to the surface being polished, which is placed over a pad. A slurry, typically containing abrasives and various chemicals, is continuously applied to the interface of the surface and pad. The pad becomes smoother over time, resulting in a lower material removal rate

(MRR). To maintain a stable polish rate, pads need to be conditioned at regular interval, which is done using a diamond conditioner [1, 2]. Typically, Ni bonds are used to bind the diamond material to the conditioner surface. Highly corrosive slurries dissolve the nickel material used in the CMP process, leading to diamond debonding from the conditioner surface. This is detrimental to the CMP process, as it generates scratches on the metal surface. Hence, the Ni layer needs to be modified with suitable coatings to protect the surface from corrosion.

One convenient method to modify the metal surface in order to protect it from being corroded in harsh environments is the used of self-assembled monolayers (SAMs). These monolayer films can be deposited through a chemical reaction between the substrate and precursors [3]. Preparation of SAMs on substrates is of great interest due to their characteristics, which include (i) high durability due to the fact that films are chemisorbed onto the substrate through covalent bonds, (ii) nanometer-scale control of the thickness of the adsorbed films on the substrate by selecting suitable adsorbates, and (iii) the high density of the packed films [4,5].

The preparation of SAMs on solid substrates can be performed using either liquid or vapor media. Although liquid SAM (L-SAM) deposition is simple and relatively cheap, the main disadvantage associated with this method is the lack of repeatability and reproducibility, as the process is difficult to control [6,7]. On the other hand, vapor SAM (V-SAM) processing is easy to control and can be used to deposit multiple samples simultaneously [8,9]. Various systems such as organosilicon on hydroxylated surfaces [10], alkanethiols (dodecanethiol, octanedecanethiol) on Au [11,12], chlorosilanes on silicon dioxide [13], carboxylic acids on metal oxides [14], alcohols and amines on platinum [15], and alkanethiols on Cu [16,17] and Ni [18,19] have been studied in detail and reported in the literature. However, most of these studies have focused on L-SAM deposition. In the present work, SAM deposition from vapor media is considered.

In addition to V-SAM deposition, the deposition of films by plasma polymerization is performed in the present work, and the results are compared with those of V-SAM deposition. The basic principle of this technique is the formation of polymers through the reaction of plasma and a precursor, where the formed polymer is allowed to deposit on the substrate. The main advantage of film deposition by plasma polymerization is that the film deposition rate (and thereby the film thickness) can be controlled at the desired rate by physical deposition mechanisms; this is in contrast to SAM deposition methods where the film thickness is restricted to monolayer coverage only [20,21].

Though organic layer deposition on metals such as Cu and Au has been widely reported, few studies have investigated the modification of Ni surfaces with organic coatings [18,19]. In the present study, the deposition of organic precursors such as 1-dodecanethiol (DT) and perfluorodecyltrichlorosil (FOTS) from vapor media onto Ni-based substrates is considered for applications using both Cu CMP and W CMP. Both of these precursors are well-documented in the literature as corrosion coatings [11,12,22,23]. The characteristics of these coatings on Ni-based substrates in various solutions are evaluated by electrochemical techniques such as potentiodynamic polarization and electrochemical impedance spectroscopy (EIS).

2. EXPERIMENTAL

The SAM formation process was carried out in a V-SAM system (AVC-100M, Sorana, Korea) at optimum conditions (a pressure of 0.5 torr and a temperature of 100°C). The detailed experimental procedure is described in our previous paper [24]. Similarly, fluorocarbons are deposited on the substrate in a PE-CVD system (SRN-504, Sorana, Korea). PECVD was conducted using C_4F_8 as a precursor gas at a 5 sccm flow rate at 150 mtorr working pressure and 150 W plasma power. The deposition time was varied according to the film thickness. For both the organic layer deposition and characterization, Ni substrates of 2 cm x 2 cm were used. Before deposition, Ni coupons were cleaned in an IPA solution with megasonic irradiation and then dried using N_2 . Electrochemical measurements such as potentiodynamic polarization and electrochemical impedance spectroscopy (EIS) were carried out to characterize the organic coating. All electrochemical measurements were carried out using a conventional three-electrode cell using a potentiostat (VersaSTAT, Princeton Applied Research, USA). The working electrode was Ni coated with different films, while the reference and the counter electrodes were Ag/AgCl (saturated KCl) and platinum mesh, respectively. Prior to the electrochemical measurements, the open circuit potential (OCP) was measured for a period of 5 minutes to allow the system to reach its steady state OCP value. A potentiodynamic polarization curve was obtained by sweeping the electrode potential from -0.25 to 0.50 V versus OCP. Impedance spectra were acquired in the frequency range of 100 kHz- 10 mHz at OCP with an AC amplitude of 10 mV rms. Commercial software (Zsimpwin) was used to estimate the EEC parameters. Contact angle measurements (Phoenix 300 plus, SEO, Korea) were also conducted to ascertain the structural integrity of the coatings. In the present work, the performance of these organic coatings against corrosion in various media such as an aqueous solution (0.1 M $NaClO_4$, pH = 7.1), a commercial Cu slurry (pH = 6.8), and a commercial W slurry (pH = 2.5) were evaluated.

3. RESULTS AND DISCUSSION

Vapor phase self-assembled monolayers (V-SAM) of two different precursors, namely DT and FOTS, were prepared on the Ni substrate. Figure 1 shows the potentiodynamic polarization curve of bare Ni and Ni coated with different films. The estimated corrosion potential and corrosion current values from these plots are given in Table 1. It is clear from Table 1 that the I_{corr} value decreases when V-SAM layers are prepared on the Ni surface. This result indicates that both coatings suppress the corrosion of the underlying Ni surface by acting as a barrier between the metal and electrolyte solution. It is also clear that the E_{corr} value of the coated surface is lower when compared to the uncoated Ni surface. It has been reported in the literature that if there is a passivation layer or thin film on the electrode surface, E_{corr} increases with decreasing I_{corr} due to the retardation of the anodic reaction (anodic dissolution of copper in the given aqueous solution) [25,26]. However, according to potential theory, this is true only if the cathodic reactions remain unaffected [27]. If the cathodic reaction (cathodic reduction of dissolved oxygen) are also affected by the formation of film on the surface, then the OCP value would either increase or decrease [28].

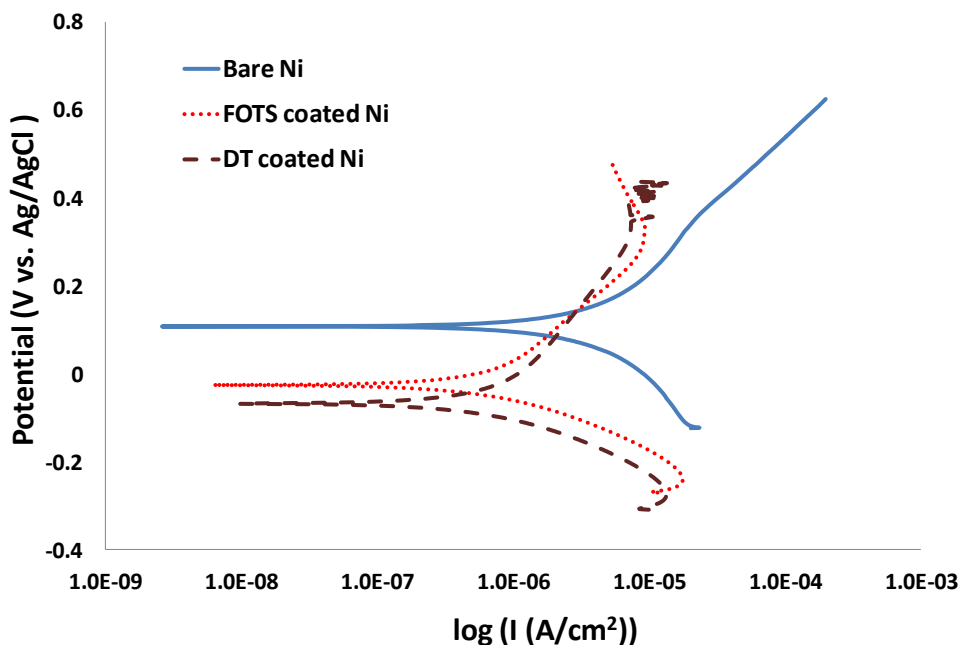


Figure 1. Potentiodynamic polarization curves of V-SAM-coated and uncoated Ni in a 0.1 M NaClO₄ solution

Table 1. Values of E_{corr} and I_{corr} .

Surface	E_{corr} , V	I_{corr} , nA/cm ²
Ni	0.107	7041
FOTS-coated Ni	-0.025	941
DT-coated Ni	-0.068	986

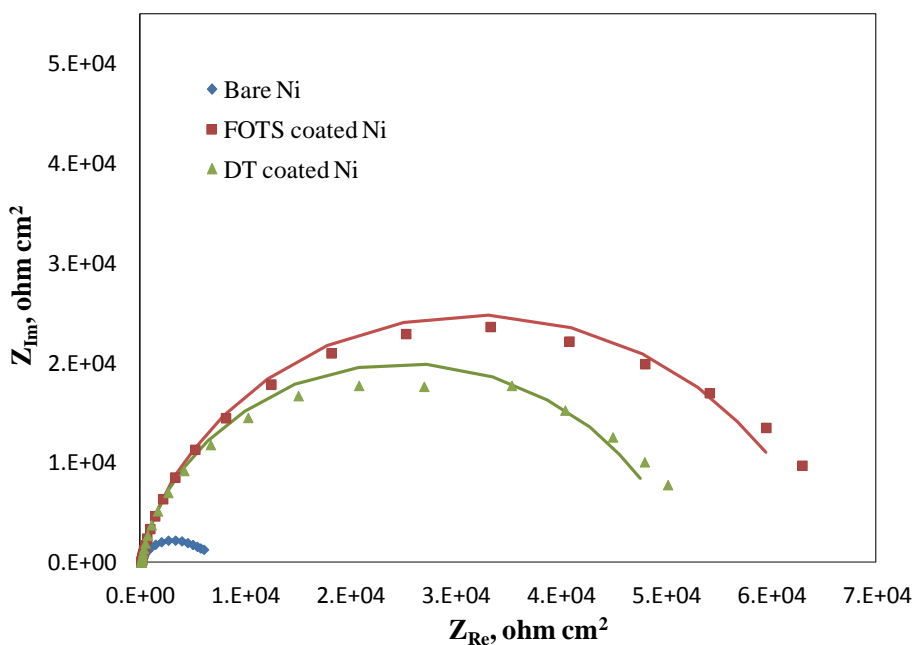


Figure 2. Simulated impedance data superimposed with experimental data of coated and uncoated Ni in a 0.1 M NaClO₄ solution.

For the FOTS and DT coating, the observed decrease in both the E_{corr} and I_{corr} values indicates that both anodic and cathodic reactions are inhibited, though there is a significantly greater reduction in the cathodic reaction rates. Similar kind of trend is also reported in the literature [4]. When compared to DT, the FOTS coating showed lower E_{corr} and I_{corr} values, which indicates that the FOTS coating has higher protection efficiency. To investigate this further, EIS measurements were conducted, and the results are shown in Figure 2.

The total impedance of each of the coated surfaces is higher than that of a bare Ni surface, which implies that both coatings provide good protection for the underlying Ni surface against corrosion. The impedance data are modeled using electrically equivalent circuits (EEC). The EEC circuit shown in Figure 3a is used to model the acquired impedance spectrum of bare surface, where R_s represents the solution resistance, Q_1 represents a constant phase element to model non-ideal capacitive behavior of the electrical double layer, and R_1 represents the polarization resistance of the bare Ni surface against corrosion reactions. Similarly, the circuits shown in Figures 3b and 3c are used to model the impedance spectrum of a coated surface under varying conditions where, R_s , Q_1 and R_1 have the same meaning as defined before, while R_2 represents the pore resistance of the coated metal and Q_2 represents the non-ideal behavior of the coating capacitance. The EEC shown in Figure 3b is used when SAM-covered metals have defects such as pin holes, and the circuit shown in Figure 3c is used when the value of R_2 is much higher than that of R_1 [4]. Since the formation of films on the metal will affect both R_1 and R_2 values [29], the summation of both of these is used to estimate the polarization resistance of coated surfaces against corrosion. The corrosion protection of the SAM coating was calculated using the following equation [5,12]:

$$Corrosion\ protection\ efficiency = \frac{(R_{coating} - R_{ref})}{R_{coating}} (\%)$$

The estimated EEC parameters of the impedance spectrum (Figure 3) are given in Table 2. The low capacitance and high resistance value of the coating surface clearly shows that the corrosion resistance of bare Ni in an aqueous solution is highly enhanced with SAM layers. Corrosion protection efficiencies of the DT and FOTS coated Ni were found to be 87% and 90%, respectively.

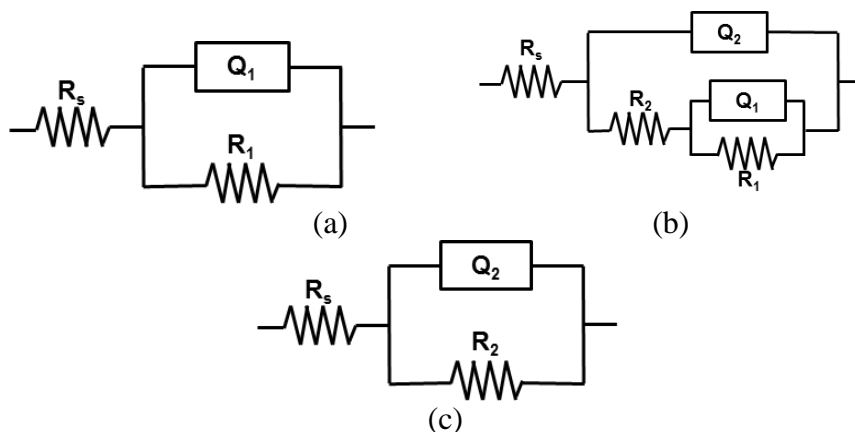


Figure 3. Electric equivalent circuits used to model the impedance data of bare Ni (a) and coated Ni (b) and (c) in various solutions.

Table 2. EEC parameters of V-SAM coated and uncoated Ni in a 0.1 M NaClO₄ solution.

Circuit parameters	Bare Ni	FOTS-coated Ni	DT-coated Ni
R _s , ohm cm ²	114	112	111
Y _{o1} , S sec ⁿ	2.2e-5	1.5e-5	2.8e-5
n ₁	0.85	0.64	0.78
R ₁ , ohm cm ²	5968	4.20e4	2.78e4
Y _{o2} , S sec ⁿ	--	1.8e-5	1.5e-5
n ₂		0.92	0.93
R ₂ , ohm cm ²	--	2.3e4	2.2e4

The efficiency of these coatings in suppressing corrosion of Ni in a commercial Cu CMP slurry was investigated. Figure 4 shows the potentiodynamic polarization curves of coated as well as uncoated Ni in a commercial Cu slurry solution. Since the anodic regions of the curves exhibit kinks at lower overpotentials, the estimation of E_{corr} and I_{corr} values through Tafel analysis would not be more accurate. However, in the qualitative analysis, both E_{corr} and I_{corr} values were decreased due to the coating surfaces, as observed in the case of aqueous solution. This implies that both the anodic and cathodic reaction rates are suppressed at the coating surface. Similar trends were observed with SAM coatings on a copper surface [4].

Figure 5 shows impedance data for both coated and uncoated surfaces. It is obvious from these figures that the total impedance of the system is significantly higher for the coated surface when compared to the uncoated Ni. Moreover, the impedance of coated surfaces measured in a Cu slurry is higher than that measured in a NaClO₄ solution. This can be attributed mainly to the presence of corrosion inhibitor in the slurry. Using the polarization resistance values shown in Table 3, the corrosion protection efficiency was estimated as 98% and 96.5% for FOTS and DT, respectively.

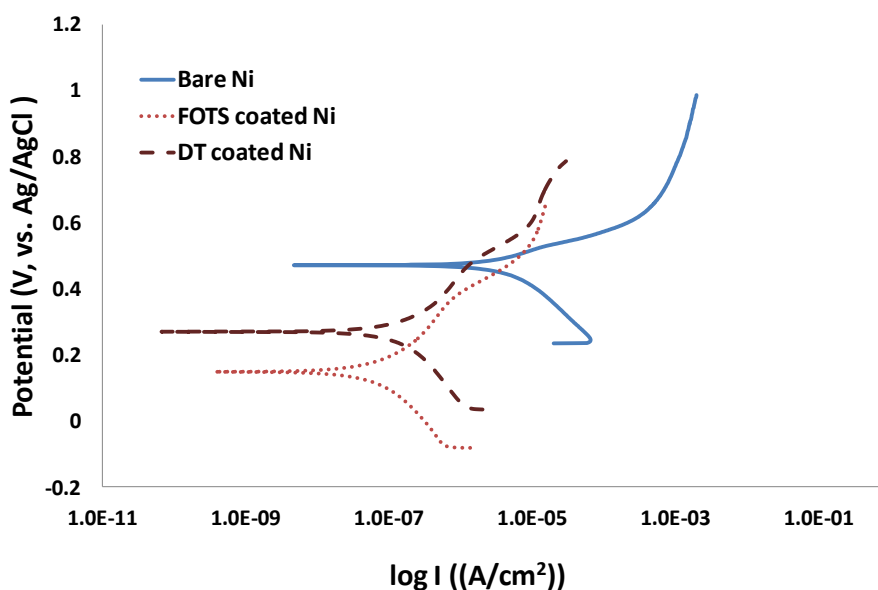


Figure 4. Potentiodynamic polarization curves of V-SAM-coated and uncoated Ni in a commercial Cu slurry.

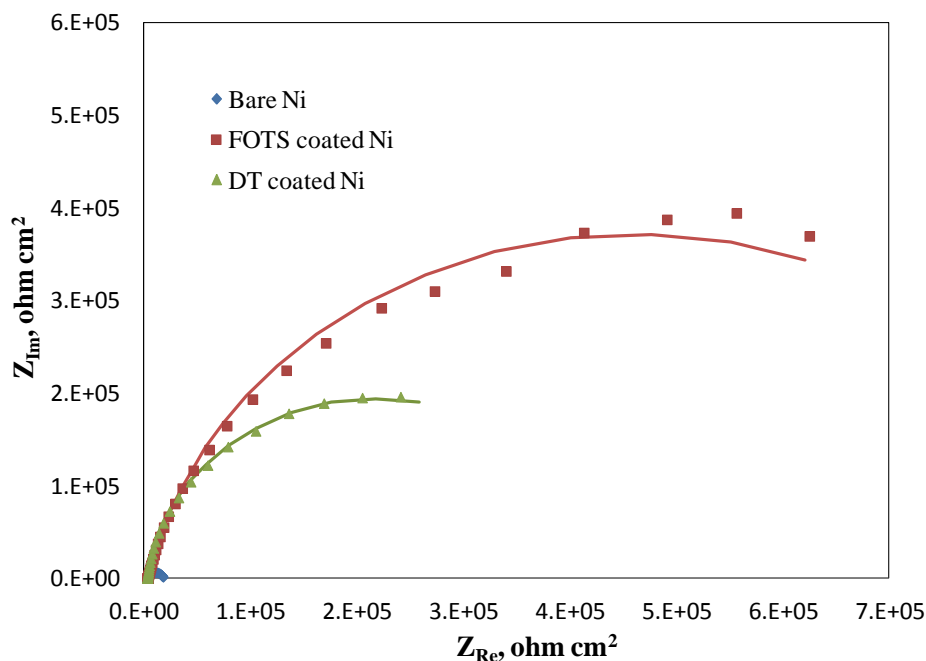


Figure 5. Simulated impedance data superimposed with experimental data of V-SAM-coated and uncoated Ni in a commercial Cu slurry.

Table 3. EEC parameters of V-SAM coated and uncoated V-SAM coated and uncoated Ni in a commercial Cu slurry

Circuit parameters	Bare Ni	FOTS-coated Ni	DT-coated Ni
$R_s, \text{ohm cm}^2$	3439	3569	3320
$Y_{o1}, \text{S sec}^n$	1.1e-5	--	--
n_1	0.91	--	--
$R_1, \text{ohm cm}^2$	1.5e4	--	--
$Y_{o2}, \text{S sec}^n$	--	4.3e-6	5.5e-6
n_2	--	0.87	0.93
$R_2, \text{ohm cm}^2$	--	9.2e5	4.3e5

Though the suggested coated Ni surfaces show good corrosion resistance against Cu slurry, the effectiveness in terms of corrosion resistance was also tested in a highly acidic W CMP slurry (pH = 2.5). Figure 6 shows the potentiodynamic polarization curves of bare metal and SAM coated Ni surfaces in a commercial W slurry. It is evident that there is no significant change in the polarization curves between coated and uncoated metal surfaces, which indicates that the deposited coatings could not provide adequate protection to the underlying metal surfaces when in contact with the W slurry. This might be due to the highly acidic W slurry delaminating the coating along with the underlying Ni. Mekhalif et al.[18] reported that the adhesion strength of DT is lower when it is deposited from a liquid media on an untreated Ni surface, as the native oxide present on the Ni surface interferes with the chemical reaction between the DT and Ni substrate. That is, the thiols in the precursor oxidize into sulfonates and sulfinates, resulting in coatings of poor quality. Although the V-SAM coating on Ni

shows good protection efficiency in a commercial Cu slurry, the presence of defects in the V-SAM due to the poor adhesion strength between the organic layer and the Ni surface might allow slurry to pass through the SAM defects (pin holes), resulting in contact with the underlying Ni substrate. Being highly acidic, the W slurry eventually etches the SAM-coated Ni. Though, we observed the protection efficiency is slightly higher with FOTS-deposited Ni, the dissolution rate of VSAM-coated Ni substrates is still high in highly acidic W slurry. Contact angle measurements were carried out on both V-SAM-covered Ni surfaces and bare Ni before and after dipping in a W slurry for one minute to corroborate the electrochemical results. As expected, the contact angle decreases to less than 5° from the original values of 78° and 110° for DT and FOTS, respectively (refer to Table 4).

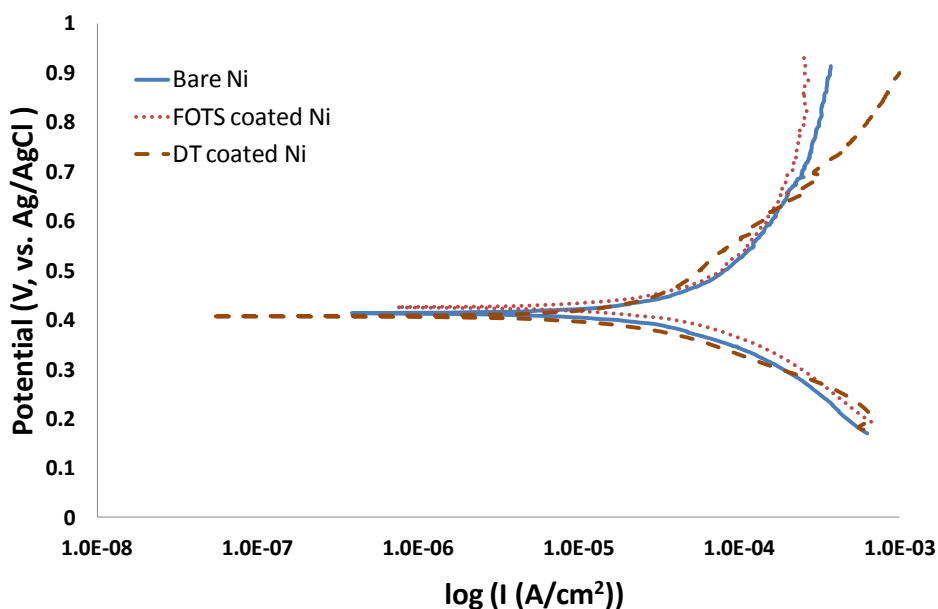


Figure 6. Potentiodynamic polarization curves of V-SAM-coated and uncoated Ni in a commercial W slurry.

Table 4. Contact angle measurements of bare and coated Ni before and after dipping in W slurry for one minute.

Surface	Contact angle, degree	
	Before dipping in W slurry	After dipping in W slurry for one minute
Ni	31	<5
FOTS-coated Ni	110	<5
DT-coated Ni	78	<5

Mekhalif et al. suggested the use of electrochemical pretreatment of Ni to remove native oxides from the surface in order to increase the quality of coatings [18]. However, in the present work, we chose a Ni alloy, a mixture of palladium-nickel-chrome (PNC), to improve the quality of the coating films, as the electrochemical resistance of PNC to oxidation is higher than that of a bare Ni surface.

The organic films were deposited on the PNC by the same procedure, and the coating characteristics were evaluated through electrochemical analysis. Figures 7 and 8 show the potentiodynamic polarization and impedance curves of bare and coated Ni alloys in a commercial W slurry. Figure 7 clearly shows that the V-SAM-coated Ni alloy substrates have higher corrosion resistance than V-SAM-coated Ni in a W slurry. It should also be noted that, unlike on Ni, the E_{corr} value increases with V-SAM coatings on PNC. This is mainly due to the inhibition of anodic reactions with V-SAM coatings on the PNC surface. The EEC parameters derived from the impedance data are given in Table 5, and the corrosion protection efficiency of DT- and FOTS-deposited PNC was further increased to 48 and 74%, respectively. The higher corrosion protection efficiency can mainly be attributed to the higher corrosion resistance of PNC itself. Hence, VSAM-deposited PNC could be the better choice for W CMP applications.

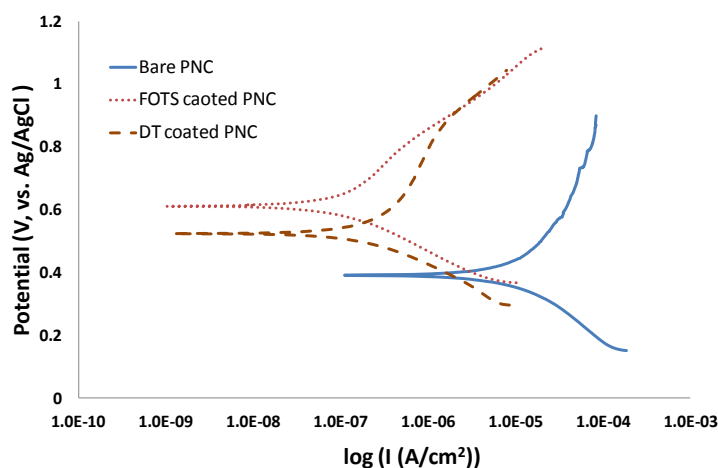


Figure 7. Potentiodynamic polarization curves of V-SAM-coated and uncoated PNC in a commercial W slurry.

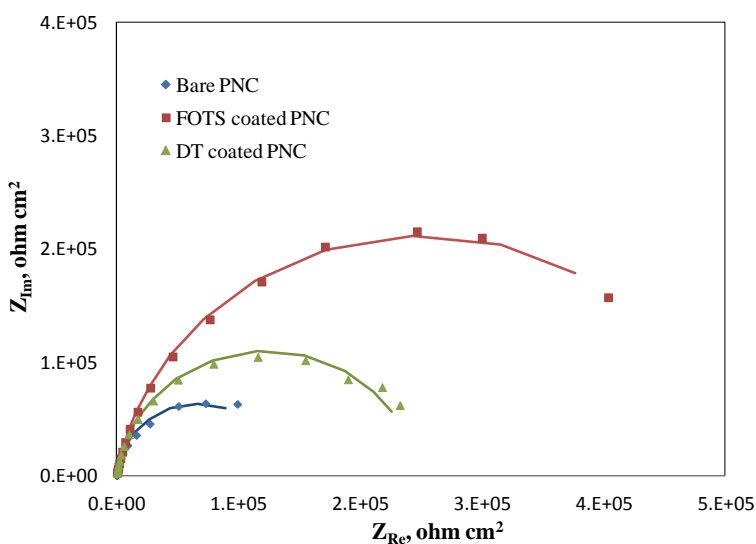


Figure 8. Simulated impedance data superimposed with experimental data of V-SAM-coated and uncoated PNC in a commercial W slurry.

Table 5. EEC parameters of V-SAM-coated and uncoated PNC in a commercial W slurry.

Circuit parameters	Bare PNC	FOTS-coated PNC	DT-coated PNC
$R_s, \text{ohm cm}^2$	97.5	92.7	98.5
$Y_{o1}, \text{S sec}^n$	$6.1e-7$	--	--
n_1	0.96	--	--
$R_1, \text{ohm cm}^2$	$1.3e5$	--	--
$Y_{o2}, \text{S sec}^n$	--	$1.4e-7$	$1.3e-7$
n_2	--	0.89	0.93
$R_2, \text{ohm cm}^2$	--	$5.0e5$	$2.5e5$

The deposition of fluorocarbons of various thicknesses (50 nm and 100 nm) on both Ni and PNC by a plasma polymerization technique was also conducted, and the results of the analyses of these surfaces are shown in Figure 9.

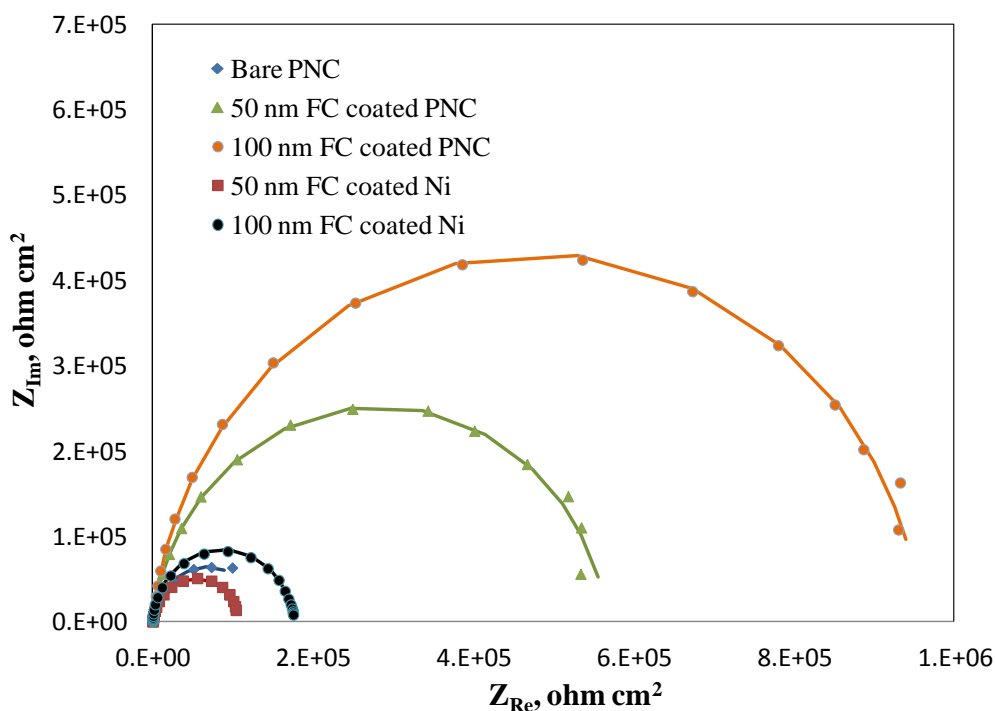


Figure 9. Simulated impedance data superimposed with experimental data of fluorocarbon-coated (by plasma polymerization) and uncoated Ni and PNC in a commercial W slurry.

The results show that, with FC films, the total impedance increases with film thickness. When compared to V-SAM deposition, FC deposition on PNC seems to be much more effective in resisting corrosion in a W slurry. Table 6 shows the EEC parameters retrieved from the Nyquist plots. For the FC-deposited PNC, the protection efficiency increases to up to 86.5% as a function of film thickness. Since this sample was subjected to plasma polymerization, the surface coverage is not restricted to a monolayer, and the formation of defects could be minimized, which results in higher protection

efficiency against corrosion. Though the polarization resistance of FC-deposited Ni is lower than that of FC-deposited PNC, it is still much higher than the polarization resistance of bare Ni in aqueous solutions. Thus, V-SAM deposited on Ni alloy and FC films thicker than 50 nm deposited by PE-CVD on Ni and Ni alloys could be the better choice for the W CMP process.

Table 6. EEC parameters of fluorocarbon-coated and uncoated Ni and PNC in a commercial W slurry.

Circuit parameters	Bare PNC	50 nm FC-coated PNC	100 nm FC-coated PNC	50 nm FC-coated Ni	100 nm FC-coated Ni
R_s , ohm cm^2	97.5	98	92	87.8	82.3
Y_{o1} , S sec^n	6.1e-7	--	--	--	--
n_1	0.96	--	--	--	--
R_1 , ohm cm^2	1.3e5	--	--	--	--
Y_{o2} , S sec^n	--	1.3e-7	5.7e-8	8.5e-8	2.9e-8
n_2	--	0.92	0.93	0.94	0.98
R_2 , ohm cm^2	--	5.7e5	9.6e5	1.1e5	1.7e5

4. CONCLUSION

The deposition of DT and FOTS on Ni substrate using the vapor phase method was studied. Electrochemical analyses reveal that the corrosion protection efficiency of FOTS is higher than DT both in aqueous solution and in a commercial Cu slurry. However, when a highly acidic W slurry is used, both these coatings show poorer performance. This is presumably due to the dissolution of coating along with the underlying Ni. Hence, a Ni alloy of palladium-nickel-chrome with organic coatings is suggested for highly acidic solutions, as this Ni alloy has a higher electrochemical resistance to oxidation when compared to Ni. The organic coatings were also deposited on Ni-based substrates by a plasma polymerization technique, and their coating characteristics were compared with V-SAM-deposited Ni substrates. In the plasma polymerization technique, the coating thickness can be controlled through the deposition rate, and the substrate with the thicker coating (100 nm) showed better performance than the V-SAM coatings.

ACKNOWLEDGEMENTS

This work was supported by the research fund of Hanyang University (HY-2011-G).

References

1. Y. Li: *Microelectronic Applications of Chemical Mechanical Planarization*, Wiley, New York (2008)
2. W. Li, D. W. Shin, M. Tomozawa, and S. P. Murarka, *Thin Solid Films*, 270 (1995) 601
3. Y.X. Zhuang, O. Hansen, T. Knieling, C. Wang, P. Rombach, W. Lang, W. Benecke, M. Kehlenbeck, and J. Koblitiz, *J. Microelectromech. Syst.*, 16 (2007) 1451

4. G. Li, H. Ma, Y. Jiao and S. Chen, *J. Serb. Chem. Soc.*, 69 (2004) 7914
5. Ž. Petrović, M. M-Hucović and R. Babić, *Prog. Org. Coat.*, 61 (2008) 1
6. S. C. Clear and P. F. Nealey, *J. Coll. Interf. Sci.*, 123 (1999) 238
7. R. Maboudian, W.R. Ashurst, and C. Carraro, *Tribol. Lett.*, 12 (2) (2002) 95
8. M. Beck, M. Graczyk, I. Maximov, E.L. Sarwe, T.G.I. Ling, M. Keil, and L. Montelius, *Microelectron. Eng.*, 61-62 (2002) 441
9. A.Y. Fadeev and T.J. McCarthy, *Langmuir*, 16 (2000) 7268
10. Z. Feng and E. Cha, Patent no. US7327535 (2008)
11. H.O. Finklea, D. A. Snider and J. Fedyk, *Langmuir*, 9 (1993) 3660
12. D. G – Raya, R. Madueño and J. M. Sevilla, *Electrochim. Acta*, 53 (2008) 8026
13. J. Sagiv, *J. Am. Chem. Soc.*, 102 (1980) 192
14. D.L. Allara and R.G. Nuzzo, *Langmuir*, 1 (1985) 45
15. H. Sellers, A. Ulman, Y. Shnidman and J.E. Eilers, *J. Am. Chem. Soc.*, 115 (1993) 9389
16. F. Sinapi, I. Lejeune, J. Delhalle and Z. Mekhalif, *Electrochim. Acta*, 52 (2007) 5182
17. K-M. Yin and H.Z. Wu, *Surf. Coat. Tech.*, 106 (1998) 167
18. Z. Mekhalif, J. Riga, J._J. Pireaux and J. Delhalle, *Langmuir*, 13 (1997) 2285
19. S. Noël, F. Houzè, L. Boyer, Z. Mekhalif, J. Delhalle and R. Cuadano, *IEEE Trans. Compon. Packag. Technol.*, 22 (1999) 79
20. Y. Matsumoto and M. Ishida, *Sensors and Actuators*, 83 (2000) 179
21. K. Takahashi, A. Itoh, T. Nakamura, and K. Tachibana, *Thin Solid Films*, 374 (2000) 303
22. T. M. Mayer, M.P.D. Boer, N.D. Shinn, P.J. Clews and T.A. Michalske., *J. Vac. Sci. Technol. B*, 18 (2000) 2433
23. Y. X. Zhuang, O. Hansen and J.C. He, *J. Phys.*, 152 (2009) 012029
24. I-K. Kim, T-Y. Kwon, D-C. Kim, M-S. Park and J-G. Park, *J. Electrochem. Soc.*, 158 (2011) 1
25. T-H. Tsai and S-C. Yen, *Appl. Surf. Sci.*, 210 (2003) 190
26. T. Du, A. Vijayakumar and V. Desai, *Electrochim. Acta*, 49 (2004) 4505
27. S. Aksu, L. Wang and F.M. Doyle, *J. Electrochem. Soc.*, 150 (2003) G718
28. R. P. Venkatesh, Y. N. Prasad and S. Ramanathan, *Proc. Intl. conf. Planarization/CMP Tech.*, (2011) 374
29. A.M. Fenelon, C. B. Breslin, *J. Appl. Electrochem.*, 31 (2001) 509